DESIGN AND THERMAL ANALYSIS OF A NOVEL PERMANENT MAGNET-FRICTION INTEGRATED BRAKE FOR VEHICLE

by

Kuiyang WANG [a,b], ***Ren HE*** [a*], ***Jinhua TANG*** [a,b], ***and Ruochen LIU*** [b]

[a] School of Automotive and Traffic Engineering, Jiangsu University, Zhenjiang, China
[b] School of Automotive and Traffic Engineering, Jiangsu University of Technology, Changzhou, China

Original scientific paper
https://doi.org/10.2298/TSCI190609070W

This article focuses on a new type of permanent magnet-friction integrated brake. The design scheme of integrated brake is proposed. Taking the maximization of braking moment and the minimization of volume as the dual optimization objectives, the particle swarm optimization algorithm is used to optimize the integrated brake, and the main structure parameters of the integrated brake are obtained. Based on the obtained structure parameters, the 3-D model of integrated brake is established. The mathematical models of electromagnetic field and temperature field of integrated brake are given, respectively. Taking a typical braking process as an example, the magnetic field of integrated brake is analyzed based on COMSOL software, which verifies the correctness of the design model of permanent magnet brake. The eddy current loss in the magnetic field of permanent magnet brake and the thermal contact of friction brake are taken as heat sources of the integrated brake, then the temperature field of integrated brake is analyzed. The analysis results show that the integrated brake meets the requirements of braking performances, and improves the heat recession resistance compared with the traditional friction brake.

Key words: *automotive engineering, permanent magnet brake, friction brake, integrated brake, numerical simulation, thermal analysis*

Introduction

As the main braking mode of vehicle at present, friction braking will cause the temperature of brake to rise continuously under continuous braking or frequent braking conditions, which will lead to the heat recession phenomenon of brake in serious cases, and even cause traffic accidents [1]. The permanent magnet brake is a non-contact auxiliary brake, which can effectively share the braking load of friction brake, raise the braking performances of vehicle and the service life of friction brake. Hence, the permanent magnet-friction integrated brake will be an effective hybrid brake mode of vehicle. So far, the research on the permanent magnet-friction integrated brake has rarely been mentioned. An integrated brake, which combined friction brake with permanent magnet brake, was proposed [2-4]. Two types of electromagnet-friction integrated brakes were proposed [5, 6].

* Corresponding author, e-mail: heren@ujs.edu.cn

Structure of integrated brake

The proposed integrated brake is shown in fig. 1, which consists of permanent magnet brake and electro-mechanical friction brake. When the permanent magnet brake works, the regulating motor can drive the movable magnet bracket to rotate at a certain angle, so that the permanent magnet braking moment can be regulated by changing the magnetic flux of the integrated brake disc. When the friction brake works, the brake motor works according to the instructions of brake control unit. Through the screw nut mechanism, the friction blocks on both sides are pushed to the integrated brake disc, so as to realize the control of friction braking moment.

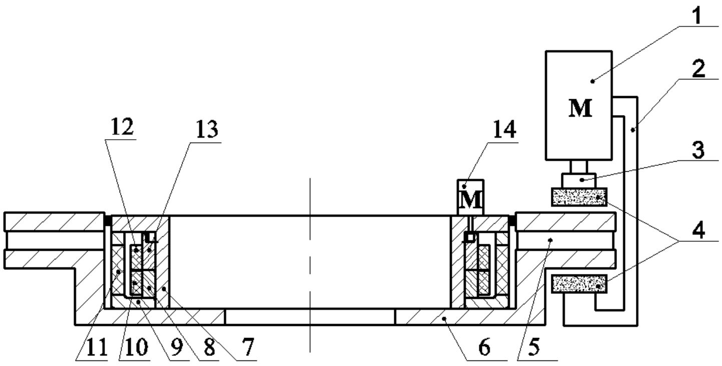

Figure 1. Structure of the permanent magnet-friction integrated brake; *1 – brake motor, 2 – caliper body, 3 – screw nut mechanism, 4 – friction block, 5 – ventilation slot, 6 – integrated brake disc, 7 – bracket race, 8 – fixed magnet bracket, 9 – magnetic circuit guide frame, 10 – fixed magnet, 11 – magnetic conductive pole sheet, 12 – movable magnet, 13 – movable magnet bracket, 14 – regulating motor*

Optimum design of structure parameters

Braking torque of integrated brake

According to [7], the braking moment equation of integrated brake may be expressed:

$$T(t) = T_{\max}(1 - \mathrm{e}^{-\beta t}) \tag{1}$$

where T_{max} is the maximum braking torque generated by the integrated brake, β – the parameter related to brake structure, and t [s] – the braking time.

Braking torque of permanent magnet brake

According to [8], the braking moment of permanent magnet brake is deduced as follows, based on the equivalent magnetic circuit method and the eddy current loss principle:

$$T_y = \frac{2\pi\sigma a r^3(\mu_0 H_c h)^2}{\left| 9l_g^2\sqrt{\frac{15\sigma\mu N_p}{\pi}}\frac{1}{\sqrt{n}} + 6K_d\mu_0\sigma b r l_g + \left(K_d\mu_0\sigma b r\right)^2\sqrt{\frac{\pi}{15\sigma\mu N_p}}\sqrt{n} \right|} \tag{2}$$

where σ [Sm^{-1}] is the conductivity of integrated brake disc, a [m] – the axial length of permanent magnet, b [m] – the circumferential length of permanent magnet, h [m] – the height of permanent magnet, r [m] – the internal radius of rotor drum in integrated brake disc, l_g [m] – the air gap between the rotor drum and the stator, μ_0 [Hm^{-1}] – the vacuum permeability, μ [Hm^{-1}] – the permeability of rotor drum, N_p – the number of magnetic pole pairs, n [rpm] – the speed of rotor drum, and K_d – the conversion coefficient of eddy current, which is usually taken as 0.6-1.2.

Braking torque of friction brake

It can be obtained easily from eqs. (1) and (2) that the braking moment of friction brake is:

$$T_f = T - T_y = \frac{T_{\max}(1-\mathrm{e}^{-\beta t}) - 2\pi\sigma a r^3(\mu_0 H_c h)^2}{\left| 9l_g^2\sqrt{\dfrac{15\sigma\mu N_p}{\pi}}\dfrac{1}{\sqrt{n}} + 6K_d\mu_0\sigma b r l_g + \left(K_d\mu_0\sigma b r\right)^2\sqrt{\dfrac{\pi}{15\sigma\mu N_p}}\sqrt{n}\right|} \tag{3}$$

According to eq. (3), it can be seen that the braking moment of integrated brake is related to the structural parameters of friction brake and permanent magnet brake. The design principle of integrated brake is to design permanent magnet brake without changing the shape size of original friction brake, and the braking moment of permanent magnet brake is mainly determined by the structure parameters of permanent magnet.

Optimization of structure parameters

The Volkswagen Teramont 2019 380TSI 4WD is chosen as the reference model. From eq. (1) and the parameters of vehicle model, it can be roughly calculated that the maximum braking moment of single wheel is about 800 Nm under high braking load. Therefore, the maximum braking moment of single-wheel permanent magnet brake should be controlled around 400 Nm to meet the requirements of practical application. The minimum total volume of permanent magnets and the maximum braking moment of permanent magnet brake are set as optimization objectives. The objective equations obtained are:

$$\begin{gathered}\min V = \min(abh), \quad \max T_y = 400 \\ \frac{\pi(r-h-g_1-g_2)}{N_p+1} \le 1.3b \le \frac{\pi(r-h-g_1-g_2)}{N_p} \\ 0 \le 2.8a \le l_w, \quad \underline{b} \le b \le \overline{b}, \quad \underline{h} \le h \le \overline{h}\end{gathered} \tag{4}$$

where V [m^3] is the volume of permanent magnet, l_w [m] – the width of rotor drum, g_1 [m] – the air gap between permanent magnet and magnetic pole cage, g_2 [m] – the air gap between rotor drum and magnetic pole cage, the range of b is [0.015, 0.05], the range of h is [0.001, 0.011].

The objective equations are optimized by particle swarm optimization (PSO) based on MATLAB software. The optimized fitness function values are obtained: the volume of permanent magnet is $6.19 \cdot 10^{-6}$ m^3, the axial length of permanent magnet is 19.1 mm, the circumferential length of permanent magnet is 38.6 mm, the height of permanent magnet is 8.4 mm, and the braking moment after optimization is 400.0001 Nm which is close to the ideal value. This shows that the optimal values of volume and braking torque of permanent magnet brake can be obtained by parameters optimization based on PSO.

Numerical simulation of electromagnetic field

Mathematical models of electromagnetic field

In the electromagnetic field model of permanent magnet brake, the displacement current in the eddy current region is neglected. Maxwell's equation can be expressed as [9]:

$$\nabla \times H = J$$
$$\nabla \times E = -\frac{\partial B}{\partial t} \tag{5}$$
$$\nabla \cdot B = 0$$

where H [Am^{-1}] is the magnetic field intensity, J [Am^{-2}] – the ampere density, E [Vm^{-1}] – the electric intensity, and B [T] – the flux density.

Simulation analysis of electromagnetic field

As shown in fig. 2, when the magnetic poles of the movable magnets are completely juxtaposed with those of the fixed magnets, the braking torque of permanent magnet brake is maximum.

The vector map of magnetic field intensity of permanent magnet brake is shown as fig. 3. When the polarity of each movable magnet is the same as that of the adjacent fixed magnet, almost all the magnetic induction lines pass through the air gap and enter the rotor drum, which is completely consistent with the theoretical analysis.

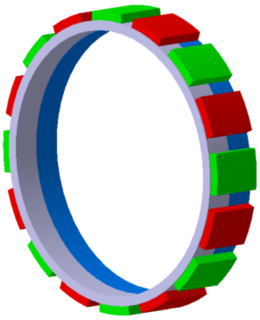

Figure 2. Permanent magnet model with maximum braking torque

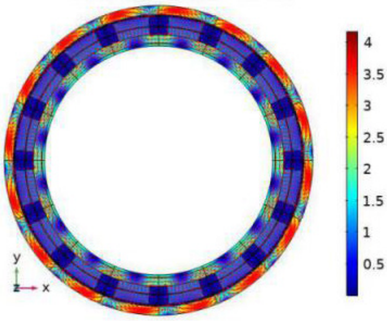

Figure 3. Magnetic field intensity of permanent magnet brake

Taking the complete braking state as an example, the transient electromagnetic fields of permanent magnet brake are calculated at different rotational speeds, and the induced eddy current density and the braking moment of permanent magnet brake are analyzed. The eddy current density distribution of rotor drum at different rotational speeds is shown in fig. 4. As the rotational speed of rotor drum decreases, the eddy current density becomes smaller and smaller. Moreover, the maximum eddy current density always concentrates on the rotor drum region corresponding to the flux output side. This shows that the maximum response magnetic field is here, and it is most likely to cause permanent magnet loss of magnetism.

When the vehicle speed is 100 km/h, the corresponding wheel speed is 94.2 rad/s, the braking moment of permanent magnet brake obtained by simulation is shown in fig. 5.

As can be seen from fig. 5, the braking moment provided by permanent magnet brake is about 400 Nm when the wheel speed is 94.2 rad/s, which is close to the theoretical calculation

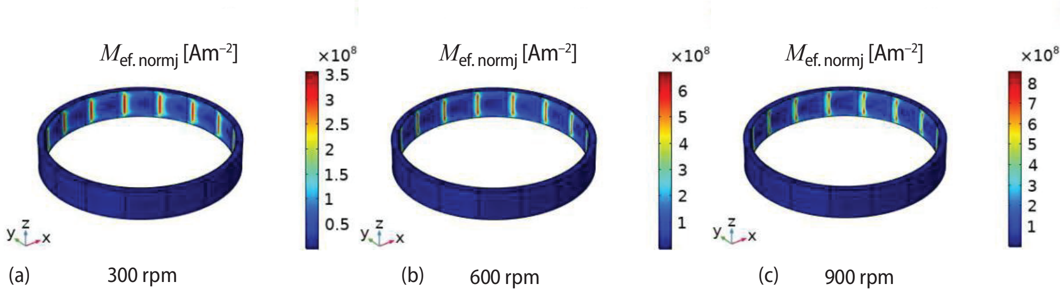

Figure 4. Eddy current density of rotor drum at different rotational speeds

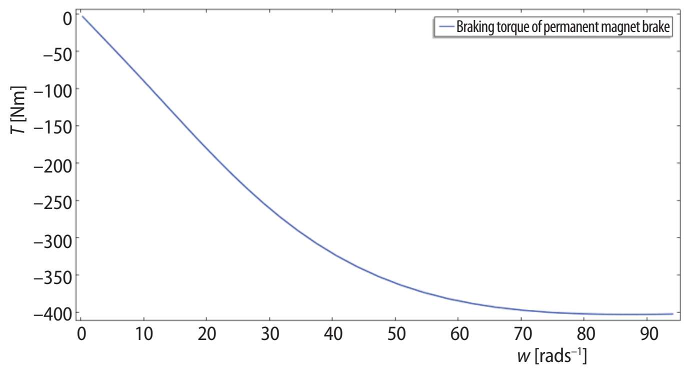

Figure 5. Characteristic curve between braking moment and wheel speed

value. When the wheel speed is greater than 62 rad/s, the braking moment is stable at about 400 Nm. With the further reduction of wheel speed, the braking moment of permanent magnet brake decreases continuously, and the permanent magnet brake gradually withdraws from work.

Numerical simulation of transient temperature field

Mathematical models of temperature field

The heat transfer within the integrated brake disc and between the contact parts is basically carried out by means of heat conduction. The basic equation is [10]:

$$Q_c = \lambda A \frac{\Delta t_m}{\delta} \tag{6}$$

where Q_c [W] is the heat flux of conduction, λ [Wm^{-1}°C^{-1}] – the heat conductivity, A [m^2] – the heat conduction area, Δt_m [°C] – the mean temperature difference of heat conduction, δ [m] – the heat conduction distance.

The heat transfer between the components and the ambient air is mainly carried out by means of heat convection and heat radiation. The basic equation is:

$$Q_d = A_s \varepsilon C_s \left(T_w^4 - T_A^4\right) + A_c h_c \left(T_w - T_A\right) \tag{7}$$

where Q_d [J] is the energy of heat conduction, A_s [m^2] – the area of heat convection, ε – the skin emissivity, C_s – the blackbody radiation constant, h_c [Wm^{-2}°C^{-1}] – the coefficient of heat convection, T_w and T_A [°C] are the surface temperature and the ambient air temperature respectively. The ambient air temperature is taken as 20 °C in this paper.

Simulation analysis of temperature field

A 3-D model of the integrated brake is established as shown in fig. 6.

The temperature rise generated by the permanent magnet brake uses the eddy current loss calculated in the electromagnetic field as heat source. The temperature rise generated by the friction brake uses the heat contact between the friction blocks and the integrated brake disc as heat source, which is calculated by using the formula of heat generation rate $Q = P/V$.

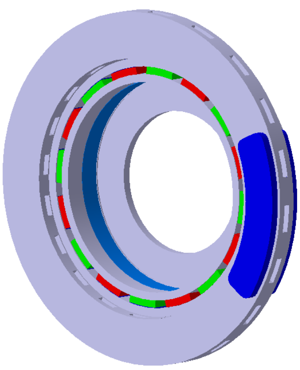

Figure 6. The 3-D model of integrated brake

Through numerical simulation, the braking states of integrated brake disc are obtained when the ambient temperature is 20 °C and the vehicle speed drops from 100 km/h (ω = = 92.15 rad/s) to 0 km/h (ω = 0 rad/s). In the simulation analysis, the permanent magnet brake works with a constant braking moment of 400 Nm. The transient temperature contours at different times are shown in fig. 7.

As can be seen from fig. 7, the area with the highest temperature is located in the friction brake part of integrated brake disc, and the area of sub-high temperature is located in the permanent magnet brake part of integrated brake disc. This shows that the temperature rise of friction brake is higher than that of permanent magnet brake. The temperature distribution of each node on the friction brake part is uneven, the temperature of the place where the friction blocks and the integrated brake disc have just rubbed is obviously higher than that of the part which is going to enter into friction. This is because the temperature of friction brake disc rises rapidly under the action of friction when the nodes of friction brake disc pass through the contact area with the friction blocks. When the nodes are separated from the friction blocks, the temperature of nodes begins to decrease due to the influence of heat convection and heat conduction. The high temperature area of the inner surface of integrated brake disc is mainly the distribution area corresponding to the permanent magnets. The temperature distribution of each node in this region is more uniform. The part near the friction brake disc is affected by the radiation of friction heat, and the temperature of this part rises slightly, but the difference is not significant. The temperature curves of friction brake part and permanent magnet brake part of integrated brake disc with time are shown in fig. 8.

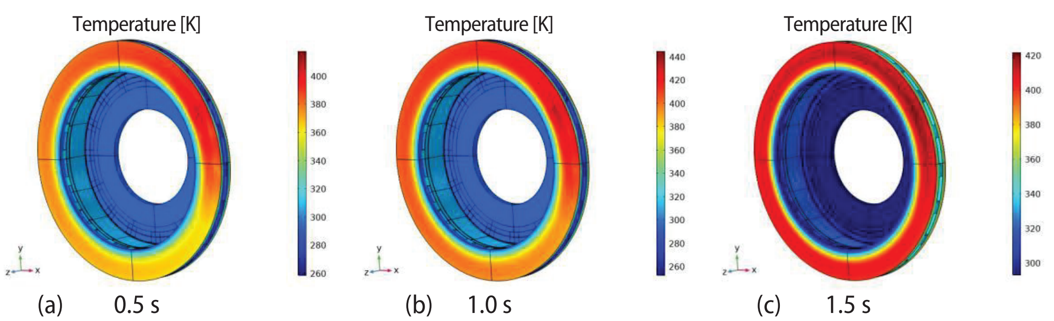

Figure 7. Transient temperature contours at different times

As can be seen from fig. 8, during the whole braking process, the temperature rise of friction brake is obviously higher than that of permanent magnet brake. This is because the friction brake is contact brake, so the temperature rise is obvious, while the permanent magnet brake is non-contact brake, the temperature rise during the whole braking process is low. In the initial stage of braking, the maximum temperature of integrated brake disc rises rapidly with time, because the heating power of integrated brake disc caused by braking energy is larger than its heat dissipation power. The temperature of friction brake reaches 440 K at 0.9 seconds and that of permanent magnet brake reaches 322 K at 1.1 seconds. Thereafter, with the decrease of vehicle speed, the heating power is less than the heat dissipation power. The maximum temperature decreases gradually and after a braking cycle, the maximum temperature of friction brake is 370 K and the maximum temperature of permanent magnet brake is 318 K. Because the temperature of permanent magnet brake rises slowly in a short time, the effect of permanent magnet brake on friction brake under emergency braking condition is negligible. Moreover, the temperature transfers from high temperature to low temperature, and the temperature rise of friction brake is faster than that of permanent magnet brake, so the effect of permanent magnet brake on the temperature rise of integrated brake is very small.

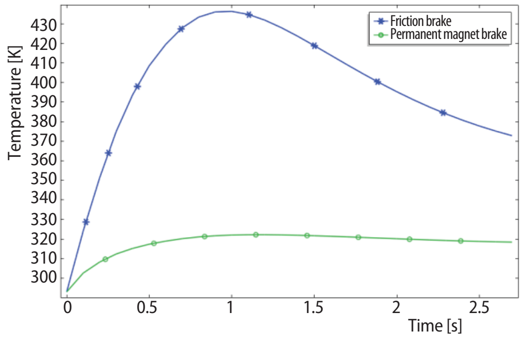

Figure 8. Temperature curves of integrated brake disc with time

The temperature distribution of brake disc is compared between the traditional disc brake and the integrated brake proposed in this paper. The maximum temperature curves of the traditional friction brake disc and the integrated brake disc under emergency braking condition are shown in fig. 9.

It can be seen from the fig. 9 that the maximum temperature rise of integrated brake disc is obviously lower than that of traditional friction brake disc. The maximum temperature of integrated brake disc is 440 K, while that of traditional friction brake disc is 550 K, the temperature rise is decreased by 37.5%. Therefore, the proposed integrated brake is reasonable and feasible, which can effectively reduce the thermal decay of vehicle brake and improve the performances of vehicle brake.

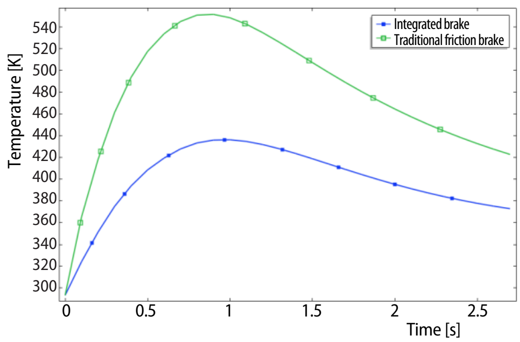

Figure 9. Contrast curves of temperature rise between two different brakes

Conclusion

A new type of brake integrated by permanent magnet brake and friction brake is proposed. The structure parameters of integrated brake are obtained by PSO, and the mathematical models of integrated brake are established. The electromagnetic field and temperature field of integrated brake are analyzed based on finite element method. Compared with the traditional friction brake, the temperature rise of new integrated brake is significantly lower than that of the traditional friction brake, which effectively improves the heat recession resistance of brake. These lay a theoretical foundation for subsequent prototype fabrication and performance tests.

Acknowledgment

This work was jointly supported by the National Natural Science Foundation of China (grants 51705221); the National Natural Science Foundation of China (grants 51875258); Research & Innovation Foundation of General University Graduate of Jiangsu Province (grants CXZZ13_0659), and the Overseas Training Foundation for Universities of Jiangsu Province.

Conflicts of Interest

The authors declare no conflict of interest.

References

[1] Asif, A., Muhammad, A. M., Thermo-Mechanical and Structural Performances of Automobile Disc Brakes: A Review of Numerical and Experimental Studies, *Archives of Computational Methods in Engineering, 26* (2019), Sept., pp. 1489-1513
[2] Gay, S. E., Contactless Magnetic Brake for Automotive Applications, Ph. D. thesis, Texas A&M University, College Station, Tex., USA, 2005
[3] Lara, M., Complex Variables Approach to the Short-Axis-Mode Rotation of a Rigid Body, *Applied Mathematics & Nonlinear Sciences, 3* (2018), 2, pp. 537-552
[4] Bortolan, M. C., Rivero, F., Non-Autonomous Perturbations of a Non-Cclassical Non-Autonomous Parabolic Equation with Subcritical Nonlinearity, *Applied Mathematics & Nonlinear Sciences, 2* (2017), 1, pp. 31-60
[5] He, R., Hu, D. H., Hybrid Control Method of the Integrated System of Electromagnetic and Friction Braking of Car, *Journal of Mechanical Engineering, 52* (2016), 12, pp. 118-128
[6] Wang, K. Y., *et al.,* Performances Analysis of a Novel Electromagnetic-frictional Integrated Brake Based on Multi-physical Fields Coupling, *World Electric Vehicle Journal, 10* (2019), 9, pp. 1-16
[7] Yu, W. X., The Simulation and Analysis of the Transient Temperature Field of Automotive Disk Brake, MSc. thesis, Hefei University of Technology, 2009
[8] Zhao, X. B., *et al.,* Eddy Current Analysis and Braking Moment Calculation of Permanent Magnet Typed Eddy Current Retarder, *Journal of Machine Design, 25* (2008), 11, pp. 62-65
[9] Ye, L. Z., *et al.,* Modeling and Experimental Study of Vehicle Permanent-magnet retarder with Magneto-Thermal Coupling, *Automotive Engineering, 41* (2019), 1, pp. 103-111
[10] Su, S. C., *et al., Simulation and Design of Thermal Energy Engineering and Advanced Energy Technology*, Chemical Industry Press, Beijing, 2015

Paper submitted: June 9, 2019
Paper revised: September 6, 2019
Paper accepted: September 9, 2019